Liquid Crystal Devices for the Reconfigurable Generation of Optical Vortices

Jorge Albero, Pascuala Garcia-Martinez, Noureddine Bennis, Eva Oton, Beatriz Cerrolaza, Ignacio Moreno, *Member, IEEE, Senior Member, OSA*, and Jeffrey A. Davis, *Fellow, IEEE, OSA*

Abstract—We present two liquid crystal devices specifically designed to dynamically generate optical vortices. Two different electrode geometrical shapes have been lithographically patterned into vertical-aligned liquid crystal cells. First, we demonstrate a pie-shape structure with 12 slices, which can be adjusted to produce spiral phase plates (SPP) that generate optical vortices. Moreover, the same device can be used to generate a pseudo-radially polarized beam, by simply adding two quarter-wave plates on each side. A second device has been fabricated with spiral shaped electrodes, which result from the combination of a SPP with the phase of a diffractive lens. This device acts as a spiral diffractive lens (SDL), thus avoiding the requirement of any additional physical external lens to provide focusing of the generated optical vortices. In both devices, the phase modulation can be adjusted by means of the voltage applied to the patterned electrodes, in order to change the properties of the generated optical vortex beams. Experimental demonstrations are provided for different wavelengths.

Index Terms—Liquid crystal devices, optical vortices, spiral diffractive lenses, spiral phase plates.

I. INTRODUCTION

OPTICAL VORTICES (OV) have received much attention both for their physical insights as well as for their possible applications, for instance as elements for particle trapping [1], image processing [2], special phase contrast microscopy [3], and free-space communication [4]. The essential characteristic of a field vortex is the spiral phase profile, $\exp(i\ell\theta)$, where ℓ is the topological charge and θ denotes the azimuth angle. The most suitable way to generate an OV is by passing a fundamental mode (TEM_{00}) laser beam through an external spiral phase element, such as a computer generated hologram (CGH) [5], or spiral phase plates (SPP) [6]–[8], these showing improved efficiency. The ideal SPP has a continuous surface thickness topology that imposes the desired azimuthal phase. However, due to the fabrication limitations, SPPs usually take multilevel quantized phase values. These kinds of multilevel SPP have been fabricated using various methods, e.g., multi-stage vapor deposition process [2] or direct electron-beam writing [9]. They provide in general high efficiency, but they do not allow changing the operating wavelengths and/or topological charges. Alternatively, SPPs can be programmed onto a liquid crystal (LC) spatial light modulator (SLM) [10], [11]. SPPs displayed in such devices can be reprogrammed, but they suffer from a limited light efficiency due to the SLM pixelated structure. Each pixel consists of an active region with width w that transmits (or reflects) light, surrounded by opaque areas (dead zones) that contain control electronics and wires. There are two consequences of this structure. First, the fraction of the incident intensity that is transmitted (or reflected) is given by the fill factor $F = (w/\Delta)^2$, where Δ denotes pixel spacing. Second, the main central diffraction order has an intensity fraction proportional to the square of the fill factor or $(w/\Delta)^4$, while the rest of the intensity is spread onto other higher diffraction orders [12].

In order to avoid these effects, a LC cell was demonstrated in [13], where a specially patterned indium tin oxide (ITO) pie slices structure was created on the front side of the cell. The pie structure was made by laser lithography process using a chrome mask and then the cell was filled with LC material. That work presented the dynamic conversion of a Gaussian laser beam into a doughnut beam of topological charges of 1 and 2, with efficiency near 100%. Larger topological charge numbers have been achieved by stacking LC spiral phase plates [14]. Although the generation of OV up to $\ell = 8$ was achieved, the efficiency was reduced to 55% due to the stacking process.

Vortex beams can also be considered as circularly harmonic modes, represented by spiraling waves that also carry angular momentum. Indeed, light orbital angular momentum (OAM) has been recognized as a new promising resource for classical and quantum information applications [15], [16]. Marrucci *et al.* [16] have reported a new device named q-plate, made of a liquid crystal cell specially patterned in such a way to introduce topological charge q at the transverse plane, which is able to generate well-defined values of photons OAM. The q-plate can convert the photon spin into OAM with efficiencies up to 100% [16].

All these previous works evidence the interest in developing efficient and programmable devices for the generation and ma-

J. Albero and I. Moreno are with the Departamento de Ciencia de Materiales, Optica y Tecnologia Electronica. Universidad Miguel Hernandez, 03202 Elche, Spain (e-mail: j.albero@umh.es).

P. Garcia-Martinez is with the Departament d'Optica. Universitat de Valencia, 45100 Burjassot, Spain.

N. Bennis, E. Oton, and B. Cerrolaza are with the Departamento de Tecnologia Fotónica, Universidad Politécnica de Madrid, Madrid 28040, Spain.

J. A. Davis is with the Department of Physics, San Diego State University, San Diego, CA 92182 USA.

nipulation of vortex beams. In this work we present the fabrication of two LC devices with specific geometrical patterned electrodes, useful to generate OV of different topological charge, and with different illumination wavelengths. They are nematic type LC cells with parallel homeotropic alignment, so they act as voltage-controlled wave-plates with the phase retardance controlled via LC tilt. Two different geometrical configurations are lithographically patterned into the LC cell. The first one reproduces the classical pie-piece structure, therefore capable to generate SPPs when the voltages applied to each electrode are properly selected. The second one follows the phase pattern of the spiral diffractive lens (SDL), i.e., the phase resulting from adding the typical SPP with the phase of a diffractive Fresnel lens. The SDL focuses at a focal distance defined by the Fresnel lens, but the focalization adopts the shape of a doughnut with a size dependent on the topological charge of the SPP. SDL have been proposed for astronomical applications to allow viewing of a dim stellar object in the region of a much brighter object [17], and they have been demonstrated onto LC pixelated displays [11]. However, to our knowledge, LC devices with specific SDL electrode structures have not been reported before.

Another related area that is receiving great attention is the generation of radially polarized beams [18]. LC devices specially conceived for generating radially polarized beams have been fabricated [19], and they have also been generated with parallel-aligned LC-SLMs operating with special polarization configurations including two quarter-wave plates [20]. In this work, we apply this special configuration to convert our SPP LC cell into a device to generate pseudo-radial beams, thus avoiding the efficiency losses due to the pixelated device employed in [20]. The word pseudo-radial comes from the fact that the generated beam is not a pure radially polarized beam, but it is accompanied with a spiral phase distribution. We generate pseudo-radial beams for different wavelengths by properly adjusting the voltage to different pie sectors of the LC cell.

We organize the paper as follows: in Section 2 we analyze the theory for generating the spiral phase masks, including the SDL. In Section 3 we describe the fabrication process to generate the two LC devices here presented. The experimental realization of different vortex beams using LC SPP and LC-SDL is presented in Section 4. Finally, in Section 5 we outline the conclusions.

II. THEORY OF SPIRAL PHASE PLATES AND SPIRAL DIFFRACTIVE LENSES

The transmittance function of a conventional SPP can be represented in polar coordinates (r, θ) as

$$g(\theta) = \exp(i\ell\theta) \tag{1}$$

where ℓ is the number of 2π phase changes on the closed circle around the beam axis. Fig. 1(a) and (b) represent $g(\theta)$ for $\ell = 1$ and $\ell = 2$. However, in general, due to the limited resolution of the devices, only quantized values of the phase modulation can be produced, and multilevel SPPs must be considered. Fig. 1(c) and (d) show the quantized cases for $\ell = 1$ and $\ell = 2$, with $N = 12$ levels, as considered in our device. This quantization of the phase distribution arises other harmonic terms that create other collinear vortex beams, with different topological charges
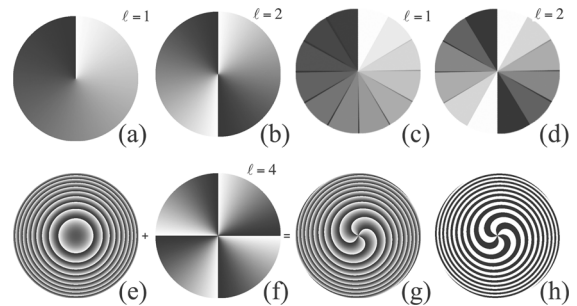

Fig. 1. Design of SPP and SLD devices. (a), (b) Continuous SPPs with $\ell = 1$, and $\ell = 2$, (c), (d) Quantized SPP with $N = 12$ and $\ell = 1$, and $\ell = 2$; (e) Diffractive lens, (f) Continuous SPPs with $\ell = 4$, (g) continuous SDL, (h) binary SDL. Gray levels denote phase values in the range $(0, 2\pi)$, except in (h) where black and white denote phases 0 and π.
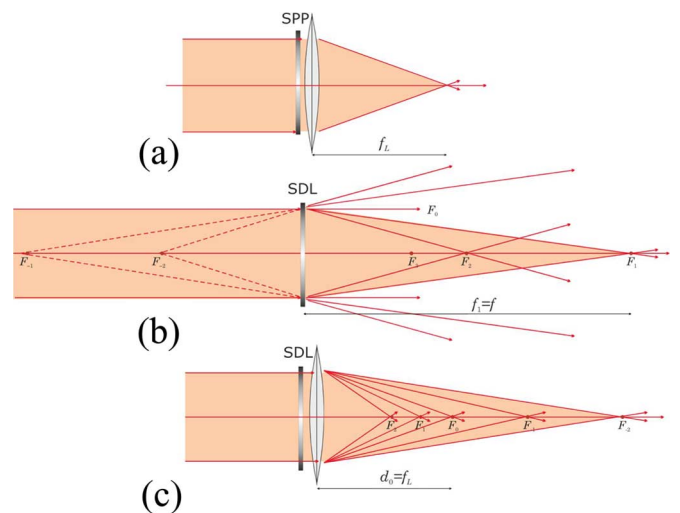

Fig. 2. Optical setups for the visualization of focused vortex beams: (a) with the SPP, (b) directly with SDL, (c) using a positive lens and SDL to visualize positive and negative harmonic terms. F_m denote the plane of focalization of the SDL harmonic order m.

[21]. The vortex beam created by the SPP mask, when focused with a physical positive lens, creates the typical doughnut of light at the back focal plane (Fig. 2(a)).

Besides, a SDL is generated by a phase-only mask defined as [11]

$$V_f(r, \theta) = \exp\left[-i\left(\frac{\pi r^2}{\lambda f} - \ell\theta\right)\right]. \tag{2}$$

where f denotes the focal length, and λ is the wavelength. Fig. 1(e) to (g) show the phases of the standard diffractive lens, a SPP with $\ell = 4$ and the resulting phase of $V_f(r, \theta)$ respectively. Finally, Fig. 1(h) shows the binary version of $V_f(r, \theta)$, binarized such that phases 0 and π are assigned to phase ranges $(0, \pi)$ and $(\pi, 2\pi)$ respectively.

In this work we fabricated this last binary SDL. The effect of such binarization is the generation of additional harmonic phase terms. The binarized version $V_f'(r, \theta)$ can be expanded as a Fourier series as [21]

$$V_f'(r, \theta) = \sum_{m=-\infty}^{+\infty} c_m \exp\left[-i\left(\frac{m\pi r^2}{\lambda f}\right)\right] \exp(im\ell\theta) \tag{3}$$

being m integer numbers and c_m the Fourier coefficients. For this type of binarization the relative intensities of each harmonic tern are $|c_m|^2 = 4/(m\pi)^2$ for odd m and zero for even m. The most efficient terms are $m = \pm 1$ and $m = \pm 3$, with relative intensities $|c_{\pm 1}|^2 = 40.5\%$ and $|c_{\pm 3}|^2 = 4.5\%$ respectively in the most intense terms. Equation (3) shows that the binarized version of the vortex lens produces the superposition of vortex harmonic lenses with topological charges $\ell_m = m\ell$ and focal lengths $f_m = f/m$.

In Fig. 2 we show the optical setups to visualize the focused vortex beams. In Fig. 2(a) a physical positive lens is placed with the SPP in order to focus the vortex beam at the back focal plane of the lens. A remarkable improvement can be achieved by using the SDL, since it substitutes both the SPP and the physical lens (Fig. 2(b)). The different harmonic terms generated by the binary SDL produce focalizations of the different vortex beams at different focal planes. The main focus is located at $f_1 = f$ and there the vortex beam with charge ℓ is focused. Note that, although the lens is binary, this focalization corresponds to a perfect continuous vortex beam. Other positive harmonic terms in (3) produce shorter focal lengths (f/m) and higher vortex charges ($m\ell$). Negative harmonic terms produce diverging beams and negative vortex charges. The DC term (zeroth order) corresponds to the light beam that remains undiffracted and shows no vortex ($\ell = 0$). These negative and DC terms can be visualized as a real pattern by simply adding a positive physical lens with short enough focal lens, as shown in Fig. 2(c).

III. FABRICATION AND CHARACTERIZATION OF SPP AND SDL DEVICES

The SPP and the SDL were both prepared with indium thin oxide (ITO) coated glass. A 12 pie-slices structure, each with an individual electrical connection, was patterned in the ITO by photolithography. A uniform ITO layer connected to the ground made the back plane of the cell. In this work, homeotropic aligned nematic liquid crystals with negative dielectric anisotropy have been used. Alignment was induced by spin-coated and rubbed alignment polyimide SE-1211 (Nissan Chemical Industries, Ltd.), specifically designed to induce vertical alignment in nematic liquid crystals. This vertical alignment (VAN) has become very interesting since the birefringence is null in absence of applied voltage. In display applications, this provides a very good dark state between crossed polarizers. For applications based on phase retardance, the phase difference is zero under the threshold voltage. Over the threshold, the liquid crystal director is reoriented by the electric field and continuous phase retardation takes place. It happens at lower voltages compared to other alignment configurations, thus leading to more stable phase values and faster switching times.

The coated substrates were rubbed in the same direction and were assembled in antiparallel orientation. The cells were filled with liquid crystal having negative dielectric anisotropy (MLC-7029 from Merck). The cell thickness was fixed about 6 μm by using silica spacers, enough to induce 2π retardation between the two orthogonal polarization states for visible wavelengths. The initial orientation of the liquid crystals is perpen-
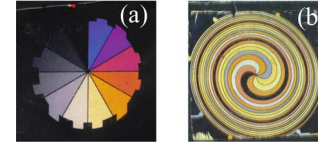

Fig. 3. Pictures of the fabricated LC cells with patterned electrodes for (a) SPP, (b) SDL.

dicular to the substrates, with a small pre-tilt to allow the molecule switching along a predefined direction. Upon application of an electric field, the molecules tilt to a horizontal position, parallel to the substrates. Different voltage can be distributed for each one of the 12 slices.

This SPP device is actually quite similar to the device reported in [13], though the former has individual addressing of each pie-slice whereas the latter uses a single pair of contacts and imposes a linear voltage distribution over the slices. Therefore, we can achieve a better adjustment of the individual voltage levels to produce the appropriate phase levels in each pie sector. In addition, cell homogeneity is not so critical to us since no voltage gradient is required.

Fig. 3 shows images of the fabricated LC cells for SPP (Fig. 1(a)) and SDL (Fig. 1(b)) when illuminated with broadband white light and placed in between linear polarizers. Arbitrary different voltages were applied to each electrode, in order to clearly visualize them. The diameter of each device is around 2.5 cm.

It is essential to apply the appropriate voltages to the electrodes in order to produce the correct phase shift for the operating wavelength and effectively create vortex beams. Therefore, we characterized the response of the LC cell for different voltages and wavelengths using a simple technique to obtain the phase retardance of a wave-plate [22]. The LC cells were placed between two parallel linear polarizers oriented at 45° with respect to the LC director axis. Then, the normalized transmitted intensity is given by

$$I = \sin^2\left(\frac{\varphi(V,\lambda)}{2}\right) \qquad (4)$$

where

$$\varphi(V,\lambda) = \frac{2\pi d}{\lambda}(n_e(V,\lambda) - n_o(\lambda)) \qquad (5)$$

is the retardance introduced by the LC layers, which depends on the wavelength (λ), and on the ordinary (n_o) and effective extraordinary (n_e) refractive indices. This last is dependent on the applied voltage (V) that causes the tilting of the LC director; d denotes the cell physical thickness.

In the experiments we employed monochromatic illumination with three different wavelengths from an Ar-Kr laser ($\lambda_R = 647$ nm, $\lambda_R = 568$ nm and $\lambda_B = 488$ nm). We measured the intensity transmitted by the polarizer—LC cell—analyzer system as a function of the applied voltage for these three wavelengths, both with parallel and also with perpendicular polarizers (this last in order to normalize the data to match the theoretical transmission in (4)). The LC cell is addressed with a square signal voltage with zero average and 1 kHz frequency. The transmission is measured versus the peak-to-peak voltage (V_{pp}), in the
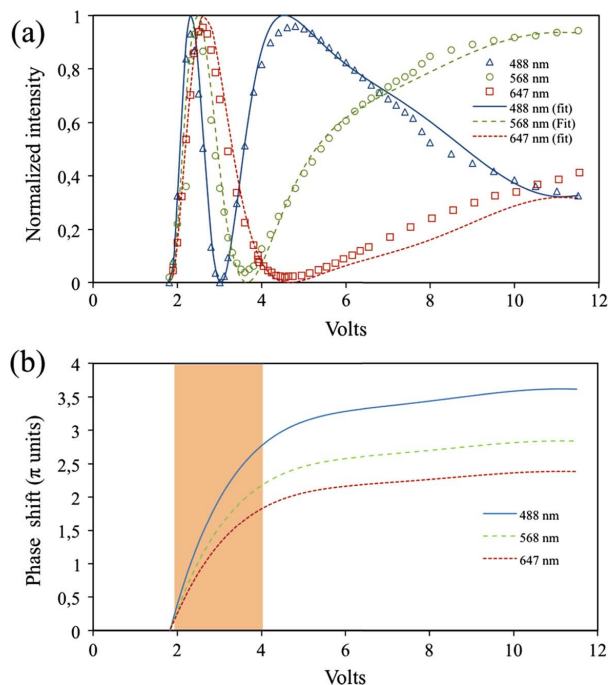
Fig. 4. Characterization of the phase retardance of the SPP LC cell, illuminating with wavelengths 647, 568 and 488 nm. (a) Experimental data (points) and the corresponding numerical fitting (lines); (b) Derived phase shift versus voltage.

range up to 10 volts. Fig. 4(a) shows the measured experimental data and the theoretical prediction after the numerical fitting of the LC retardance for the three selected wavelengths. These data follow the expected oscillatory behavior in (4). In addition, the shortest wavelength shows the fastest variation, since it produces higher values of the retardance, in agreement with (5). Fig. 4(b) shows the corresponding retardance, in units of π, obtained by fitting the data in Fig. 4(a). We imposed, in the fitting procedure, that the ratio among the retardances for the three selected wavelengths must remain fixed for all voltages. Note that, for $\lambda_B = 488$ nm, the LC cell is over 3.5π radians at the maximum applied voltage. We have chosen to operate in the voltage range between 2 and 4 volts, which produces the maximum retardance variation.

The characterization has been performed for both the SPP and the SDL devices, leading to similar results.

IV. EXPERIMENTAL GENERATION OF VORTEX BEAMS

Experimental results were obtained using these two devices. We illuminated the LC cells with the three selected wavelengths, and examined the generated diffraction pattern. We used a positive lens in order to capture the diffraction patterns at each corresponding focal plane in setups equivalent to Fig. 2(a) and (c) respectively. Diffraction patterns were captured with a colour CCD camera (Basler, model scA1390-17fc, 1392×1040 pixels), mounted on an adjustable stage.

A. Generation of Optical Vortices Using the LC SPP

We start by analyzing the generation of optical vortices using the pie shape distribution of the SPP device. In Fig. 5(a)–(c)
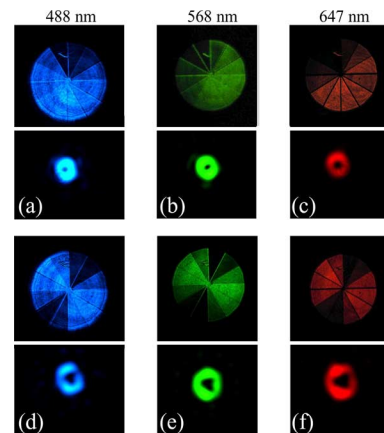

Fig. 5. Experimental realization of the $\ell = 1$ and $\ell = 2$ vortex beams with the LC SPP device with the three different wavelengths.

we analyze the case $\ell = 1$ according to twelve phase steps. For each wavelength, the twelve voltage levels were selected to produce twelve equidistant phase values between 0 and 2π across the incoming beam, First, in the upper part of the figure, we visualize the correct selection of the applied voltages, by imaging onto the camera the LC cell, placed in between the two linear polarizers oriented both at $45°$ to the LC director (and therefore selecting an intensity modulation regime, where the normalized intensity follows (4)). Note the progressive increase of the intensity. Second, in the lower part of the figures, we show the focalization of the laser beam, when the polarizers are now oriented both parallel to the LC director, in order to operate in a phase-only modulation regime. These focalizations show the characteristic doughnut shape corresponding to the vortex beam. Note that the scale of the doughnut pattern increases with wavelength, as expected.

Next, Fig. 5(d)–(f) show equivalent results to Fig. 5(a)–(c), when voltages are readjusted to generate the case $\ell = 2$. Now, two phase ramps are present in the pie-distribution. Since the LC cell does not reach 4π phase modulation, we apply voltage levels corresponding to phase values modulo 2π. Since now we are generating a larger vortex charge, the corresponding doughnut focalizations show larger diameters compared to the case $\ell = 1$.

B. Generation of Pseudo-Radially Polarized Beams Using the LC SPP

The same SPP device can be used to generate a pseudo-radially polarized beam. For that purpose, we follow the idea presented in [20], where a LC wave-plate with variable retardance is sandwiched between two quarter-wave plates (QWP), the first one oriented at $+45°$ with respect to the LC director, and the second one oriented at $-45°$. This system acts as a polarization rotator, where the rotation angle (ξ) is equal to half the phase retardation (ϕ) introduced by the LC wave-plate. Therefore, a radially polarized beam can be generated by addressing the SPP device with $\ell = 2$ (i.e., $\phi = 2\theta$), with the phase origin at the vertical direction, and selecting the input linear polarization also in the vertical orientation. Then, the polarization is rotated for every azimuth θ an angle $\xi(\theta) = \theta$, thus generating
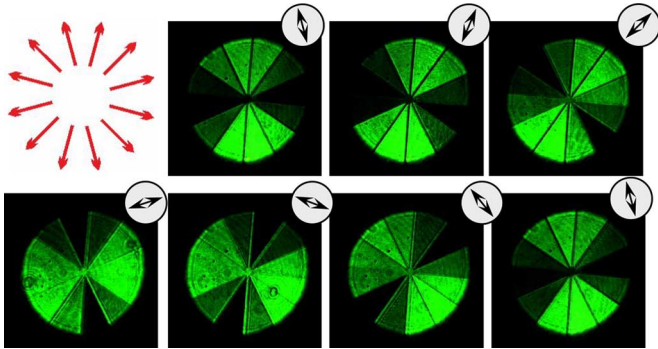
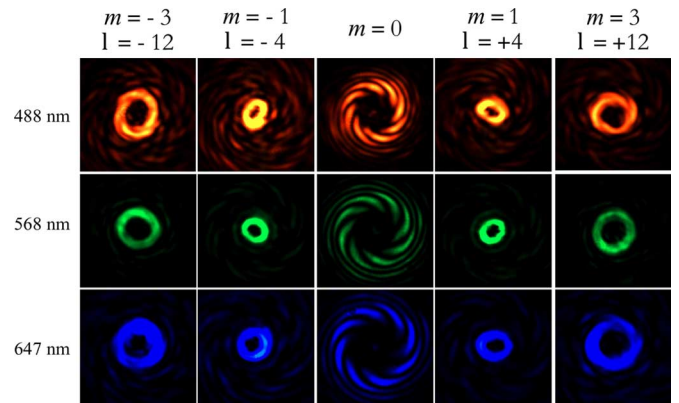Fig. 6. Experimental realization of the (pseudo) radial polarization beam.

Fig. 7. Experimental focal planes with the SDL device for the three selected wavelengths. In each case, pictures correspond to focalizations planes of $m = -3, -1, 0, +1$ and $+3$.

a (pseudo) radial polarization. As mentioned before, the radial polarization is not perfect because there is an additional phase term $\exp(i\theta/2)$ as a consequence of the polarization system. This term could be pre-compensated with a second SPP located before the optical system in order to introduce an opposite spiral phase term.

This phase term, however, is not noticeable when analyzing the state of polarization that is being created. Fig. 6 shows a sequence resulting from imaging the SPP device onto the CCD camera in the above configuration, and progressively rotating the orientation of the analyzer, which is located in front of the camera. As the analyzer rotates, the images clearly show two opposite dark sectors, where a linear polarization perpendicular to the analyzer axis is being created. The fact that these dark sectors are rotating as the analyzer is rotated, verifies the generation of the (pseudo) radial polarization beam [23].

C. Generation of Vortex Beams Using the LC SDL

Finally, we also experimentally verified the generation of optical vortices using the SDL device. From (3), this diffractive lens generates different topological charges $(m\ell)$ and focal lengths (f/m) corresponding to the different diffractive harmonic orders (m). Thus several vortices are placed within a single beam.

We used the optical system in Fig. 2(c) in order to visualize all positive and negative orders. We again employed the three wavelengths. The voltage applied to the device presented in Fig. 3(b) was adjusted to match the π phase shift at the corresponding wavelength. Then the CCD camera was placed on the different planes where vortex beams were focused. Fig. 7 shows these experimental images. As mentioned in Section 2, the phase binarization makes ± 1 and ± 3 the most intense orders. Since we encoded $\ell = 4$ in the lens, focalization of orders $m = \pm 1$ and $m = \pm 3$ reproduce vortex beams $\ell = \pm 4$ and $\ell = \pm 12$, respectively. This is verified from the greater diameter of the doughnut focalization at planes $m = \pm 3$. Since the phase retardance has been adjusted to be π radians, the zero order is absent, and the pattern on the focal plane of the physical positive lens is mainly the interference of the defocused two ± 1 orders.

It is also interesting to note that this SDL device, in addition to the encoded $\ell = 4$ charge can be used to generate $\ell = 2$, simply by assigning the same voltage to adjacent pair of electrodes.

V. CONCLUSION

In summary, we presented the fabrication of two liquid crystal devices with specific patterned electrodes, in order to produce vortex light beams. Although these kind of optical elements have been generated earlier with liquid crystal SLMs, using electrodes with specific shapes avoids other higher diffraction orders generated by the rectangular periodic structure of pixelated devices, therefore increasing the diffraction efficiency and preventing from other spurious beams. For instance, transmissive liquid crystal SLMs have fill factors in the range of 35%. Therefore, following the arguments indicated in the introduction, our non-pixelated devices imply an improvement of around 500 times greater diffraction efficiency. Modern reflective liquid crystal on silicon (LCoS) displays provide excellent fill factor values around 90%, but still a significant 1.8 factor of improvement in the efficiency is obtained.

We fabricated both, a SPP and a SDL device, using liquid crystal cells with homeotropic alignment. We presented a simple method for their calibration that permits adjusting the voltage values in order to reproduce the desired phase profiles. Experimental results demonstrate the generation of vortex beams for three different wavelengths.

REFERENCES

[1] H. He, M. E. J. Friese, N. R. Heckenberg, and H. Rubinsztein-Dunlop, "Direct observation of transfer of angular momentum to absorptive particles from a laser beam with a phase singularity," *Phys. Rev. Lett.*, vol. 75, pp. 826–829, 1995.

[2] J. A. Davis, D. E. McNamara, D. M. Cottrell, and J. Campos, "Image processing with the radial Hilbert transform: Theory and experiments," *Opt. Lett.*, vol. 25, pp. 99–101, 2000.

[3] C. Maurer, A. Jesacher, S. Fürhapter, S. Bernet, and M. Ritsch-Marte, "Upgrading a microscope with a spiral phase plate," *J. Microsc.*, vol. 230, pp. 134–142, 2008.

[4] G. Gibson, J. Courtial, M. Padgett, M. Vasnetsov, V. Pas'ko, S. Barnett, and S. Franke-Arnold, "Free-space information transfer using light beams carrying orbital angular momentum," *Opt. Exp.*, vol. 12, pp. 5448–5456, 2004.

[5] N. R. Heckenberg, R. McDuff, C. P. Smith, and A. G. White, "Generation of optical phase singularities by computer-generated holograms," *Opt. Lett.*, vol. 17, pp. 221–223, 1992.

[6] S. N. Khonina, V. V. Kotlyar, M. V. Shinkaryev, V. A. Soifer, and G. V. Uspleniev, "The phase rotor filter," *J. Mod. Opt.*, vol. 39, pp. 1147–1154, 1992.

[7] M. W. Beijersbergen, R. P. C. Coerwinkel, M. Kristensen, and J. P. Wo-erdman, "Helical-wavefront laser beams produced with a spiral phaseplate," *Opt. Commun.*, vol. 112, pp. 321–327, 1994.

[8] G. A. Turnbull, D. A. Robertson, G. M. Smith, L. Allen, and M. J. Padgett, "The generation of free-space Laguerre-Gaussian modes at millimetre-wave frequencies by use of a spiral phaseplate," *Opt. Commun.*, vol. 127, pp. 183–188, 1996.

[9] W. C. Cheong, W. M. Lee, X. C. Yuan, L. S. Zhang, K. Dholakia, and H. Wang, "Direct electron-beam writing of continuous spiral phase plates in negative resist with high power efficiency for optical manipulation," *Appl. Phys. Lett.*, vol. 85, pp. 5784–5786, 2004.

[10] M. Reicherter, T. Haist, E. U. Wagemann, and H. J. Tiziani, "Optical particle trapping with computer generated holograms written on a liquid crystal display," *Opt. Lett.*, vol. 24, pp. 608–610, 1999.

[11] K. Crabtree, J. A. Davis, and I. Moreno, "Optical processing with vortex-producing lenses," *Appl. Opt.*, vol. 43, pp. 1360–1367, 2004.

[12] J. A. Davis, J. B. Chambers, B. A. Slovick, and I. Moreno, "Wavelength-dependent diffraction patterns from a liquid crystal display," *Appl. Opt.*, vol. 47, pp. 4375–4380, 2008.

[13] D. Ganic, X. Gan, M. Gu, M. Hain, S. Somalingam, S. Stankovic, and T. Tschudi, "Generation of doughnut laser beam by use of a liquid-crystal cell with a conversion efficiency near 100%;," *Opt. Lett.*, vol. 17, pp. 1351–1353, 2002.

[14] Q. Wang, X. M. Sun, and P. Shum, "Generating doughnut-shaped beams with large charge numbers by use of liquid-crystal spiral phase plates," *Appl. Opt.*, vol. 43, pp. 2292–2297, 2004.

[15] J. P. Torres, "Quantum engineering of light," *Opt. Pura Apl.*, vol. 44, pp. 309–314, 2011.

[16] L. Marrucci, E. Karimi, S. Slussarenko, B. Piccirillo, E. Santamato, E. Magali, and F. Sciarrino, "Spin-to-orbital momentum of light and its classical and quantum applications," *J. Opt.*, vol. 13, p. 064001, 2011.

[17] G. A. Swartzlander, Jr., "Peering into darkness with a vortex spatial filter," *Opt. Lett.*, vol. 26, pp. 497–499, 2001.

[18] S. C. Tidwell, D. H. Ford, and W. D. Kimura, "Generating radially polarized beams interferometrically," *Appl. Opt.*, vol. 29, pp. 2234–2239, 1990.

[19] M. Stalder and M. Schadt, "Linearly polarized light with axial symmetry generated by liquid-crystal polarization converters," *Opt. Lett.*, vol. 21, pp. 1948–1950, 1996.

[20] J. A. Davis, D. E. McNamara, D. M. Cottrell, and T. Sonehara, "Two-dimensional polarization encoding with a phase-only liquid-crystal spatial light modulator," *Appl. Opt.*, vol. 39, pp. 1539–1554, 2000.

[21] N. Zhang, J. A. Davis, I. Moreno, D. M. Cottrell, and X.-C. Yuan, "Analysis of multilevel spiral phase plates using a Dammann vortex sensing grating," *Opt. Exp.*, vol. 18, pp. 25987–25992, 2010.

[22] P. Velásquez, M. M. Sánchez-López, I. Moreno, D. Puerto, and F. Mateos, "Interference birefringent filters fabricated with low cost commercial polymers," *Amer. J. Phys.*, vol. 73, pp. 357–361, 2005.

[23] I. Moreno, J. A. Davis, I. Ruiz, and D. M. Cottrell, "Decomposition of radially and azimuthally polarized beams using a circular-polarization and vortex-sensing diffraction grating," *Opt. Exp.*, vol. 18, pp. 7173–7183, 2010.

Jorge Albero received the Telecommunication Engineering degree from Universidad Miguel Hernández de Elche, Spain, in 2006. He received the Ph.D. degree at the Institute FEMTO-ST from the Université de Franche-Comte Besançon, France in 2010.

He was researcher pre-engineering student at the Wroclaw University of Technology for six months. During his pre-doctoral years and during his post-doctoral 12 months at FEMTO-ST he was member of the Network of Excellence on Microoptics and participated in European collaborative projects. He is currently a Researcher at Universidad Miguel Hernández de Elche under a post-doctoral scholarship from the Spanish Ministry of Educación. His research interests concern microoptics fabrication for MOEMS and integrated microscopy with spatial light modulators.

Pascuala García-Martínez received the B.S. degree in physics in 1993 and the M.S. and Ph.D. degrees in 1995 and 1998 from the University of Valencia, Spain.

She was a visiting researcher at Université Laval's Center for Optics, Photonics and Lasers under a post-doctoral scholarship from the Spanish Ministry of Education during seven months in 1999. She is currently an associate professor in the Department of Optics (University of Valencia). Dr. Garcia-Martinez's major research interests include optical and digital pattern recognition, nonlinear correlations, optoelectronic morphological image processing, optical image processing and spatial light modulators, specifically liquid crystals. She has contributed chapters to various books and she has published around fifty papers in those areas.

Dr. García-Martínez is a Member of SPIE, of the Spanish Optical Society (SEDOPTICA) and of the Spanish Royal Physical Society (RSEF). She was awarded as SPIE Senior Member in 2010, and she has been involved in SPIE Conference Committees.

Noureddine Bennis received the Ph.D. degree in physics from the University of Valencia, Spain, in 2001.

He has ample experience from his current employment in the liquid crystal group of Fotónica Aplicada in Universidad Politecnica de Madrid. He has a very long track record in manufacturing of liquid crystal displays and photonic devices based on liquid crystal technology. His experience consists of optimizing alignment conditions for smectic and nematic liquid crystal devices. Similarly he has experience in the characterization of any generic liquid crystal device.

Eva Oton received the B.Sc. degree in chemistry and the M.Sc. degree in material engineering from the Universidad Autónoma de Madrid, in 2005 and 2008, respectively.

She joined the Department of Photonic Technology in Universidad Politécnica de Madrid, Madrid, Spain. Her research interest has been focused on vertically aligned nematic liquid crystals and interaction with surface conditioning in SiOx and SiO2. She is also interested in applications of adaptive optics devices such as liquid crystal graded-index lenses and beam steering.

Beatriz Cerrolaza received the Telecommunication Engineering degree in 2006 from the Universidad Públlica de Navarra (UPNA), Spain. She received the Ph.D. degree in telecom engineering from the Universidad Politécnica de Madrid (UPM), Madrid, Spain, in 2010.

Her research interest has been focused on liquid crystal properties modelling for display and non display devices. She performed a 4 months stay at TFCG Microsystems, IMEC, Ghent in 2008 as a visiting researcher. Her main research activities during the stay consisted in the study of Motion Blur and measurement techniques of MPRT parameter.

Ignacio Moreno received the B.S. and Ph.D. degrees from the Autonomous University of Barcelona, Spain, in 1992 and 1996, respectively, both in physics.

His research interests include liquid crystal displays and its applications in diffractive and polarization optics, being coauthor of more than 90 publications in peer reviewed journals. He has been a guest scientist at various international research centers like the Department of Physics at San Diego State University, CA, the FEMTO Institut at the Université de Franche-Comté, France, and the Departamento de Física at the Universidad de la Frontera, Chile. In 2007–2011 he was the Director of the Master on Research on Industrial and Communications Engineering at the Polytechnical School in Elche (Spain).

Prof. Moreno is currently the editor of the journal Óptica Pura y Aplicada (OPA), edited by the Spanish Optical Society (SEDOPTICA). He is a Member of SEDOPTICA, SPIE and OSA. He is SPIE Senior Member and OSA Senior Member.

Jeffrey A. Davis received the B.S. degree in physics from Rensselaer Polytechnic Institute, Troy, NY, and the Ph.D. from Cornell University, Ithaca, NY.

He is currently a Professor of Physics at San Diego State University, CA, where he leads the electro-optics program. His research interests include optical pattern recognition, spatial light modulators, and programmable diffractive optical elements. He is coauthor of more than 150 publications in peer-reviewed journals

Prof. Davis is a Fellow of SPIE and the Optical Society of America.